

AGE ESTIMATION AND MASS FUNCTIONS OF TTAURI STARS IN THE TAURUS AURIGA MOLECULAR CLOUD

İ. Küçük and İ. Akkaya

Department of Astronomy and Space Sciences, Erciyes University, Turkey

Received 2009 July 10; accepted 2009 December 14

RESUMEN

En este trabajo se han calculado las funciones de masas en la actualidad (PDMF) de las estrellas T-Tauri (TTS) que están en la fase evolutiva de pre-secuencia principal (PMS) en el complejo de nubes moleculares de Taurus-Auriga. Con este fin, mediante la aplicación de nuestro código modificado de evolución estelar se utilizan modelos estelares en el intervalo de masa de $0.1 - 2.5 M_{\odot}$ para determinar la masa y la masa de edad de las TTS. La función de la masa obtenida se compara con la función de masa de Miller & Scalo (1979). La edad encontrada para las TTS es de alrededor de $1 - 3 \times 10^6$ años y la función de masa es de aproximadamente 0.644 ± 0.348 . De estos resultados, hemos calculado la tasa de formación estelar como de alrededor de $1.3 \times 10^{-7} M_{\odot} \text{ año}^{-1}$ en esta región.

ABSTRACT

In this work the present day mass functions (PDMF) of T-Tauri Stars (TTS) which are in the pre-main sequence (PMS) evolutionary phase of their evolution in the Taurus-Auriga Molecular Cloud Complex have been calculated. For this purpose, by applying our modified stellar evolutionary code, stellar models in the mass range $0.1 - 2.5 M_{\odot}$ are used to determine the mass and age mass of TTS. The obtained mass function is compared with the mass function of Miller & Scalo (1979). The age found for TTS is around $1 - 3 \times 10^6$ yr and the mass function is about 0.644 ± 0.348 . From these results, we have calculated the stellar birthrate as about $1.3 \times 10^{-7} M_{\odot} \text{ yr}^{-1}$ in this region.

Key Words: open clusters and associations: general — stars: evolution — stars: fundamental parameters — stars: pre-main sequence

1. INTRODUCTION

The stellar initial mass function (IMF), or distribution of masses with which stars are formed, is the most fundamental output function of the star formation process, and it controls nearly all aspects of the evolution of stellar systems. Young stellar clusters and groups are typical laboratories for testing theoretical stellar evolutionary models. If the stars in an open cluster are assumed to be formed at the same time, the present day mass distribution can represent the IMF of the cluster. By constructing the color-color diagrams, color-magnitude diagrams (CMDs), we can construct the initial mass function and the luminosity function (LF). These diagrams were used also for the determination of the cluster total mass and age. Since the pioneering paper of Salpeter (1955), several fundamental reviews on the Galactic

stellar mass function have been written by, in particular, Miller & Scalo (1979), and Scalo (1986). A shorter, more recent discussion is given by Kroupa (2002). Briefer reviews on the IMF have been presented by Larson (1999), Davé (2008), and Luhman (2004). During the past 50 years, the nearby Taurus-Auriga molecular cloud has become a standard region for studying low-mass star formation. Optically visible TTS data have been compared with stellar evolutionary models and good evidence has been found that stars form continuously in molecular clouds and contract down standard Hayashi tracks. Nearly all of the Taurus-Auriga pre-main-sequence stars lie within several distinct clumps of molecular gas (Kenyon & Hartmann 1995, hereafter KH95).

With far-infrared observations, we can see that young stellar objects (YSO) have some special evolu-

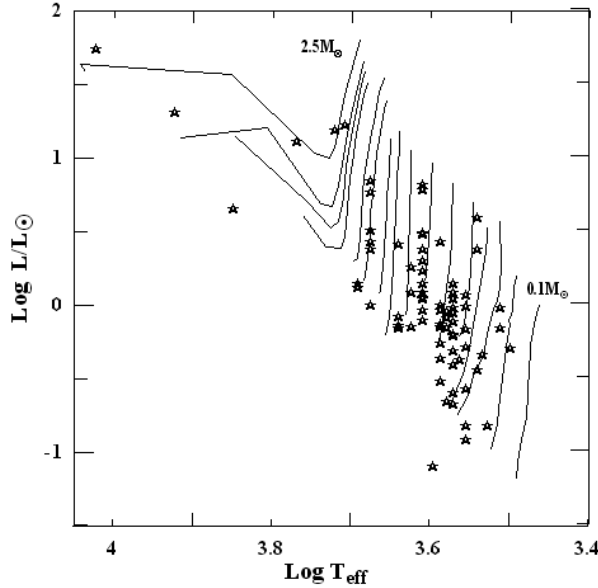


Fig. 1. Comparison to theoretical evolutionary models (Küçük et al. 1998) with TTS. The continuous lines are theoretical evolutionary path of stars having masses between 0.1, 0.2, 0.3, 0.4, 0.5, 0.6, 0.7, 0.8, 0.9, 1.0, 1.3, 1.5, 1.6, 1.8, 2.0, 2.5 M_{\odot} . TTS are shown with \star .

tionary stages before PMS evolution. These are the Class I sources, which resemble 50–100K blackbodies, with spectral energy distributions that peak at wavelengths of 30–100 μm . These optically invisible, embedded sources typically drive low velocity (stellar winds). Optically visible TTS are more numerous than Class I sources in nearby clouds like Taurus-Auriga and have a spectral energy distribution similar to that of a cool stellar photosphere. TTS can be divided into Class II and Class III sources based on their far-infrared (IR) spectral energy distribution. Class II sources display excess IR emission compared to a reddened stellar photosphere, while Class III sources display little or no excess IR emission. Classical T Tauri stars (CTTS) show strong $H\alpha$ emission lines and UV continuum excesses. Most Class III sources are weak-emission T Tauri stars (WTTS) with very weak $H\alpha$ emission and little or no UV continuum excess (Walter et al. 1988).

2. AGE AND MASS ESTIMATION OF T-TAURI STARS

If the star formation rate has been constant, the relative number of Class I sources provides an estimate of the Class I lifetime, τ_1 , if the age of typical TTS, τ_{TTS} , is also known. Using evolutionary models (Küçük et al. 1998), the derived ages are $\tau_1 = 2 - 3 \times 10^5$ yr for Class I sources and $\tau_2 =$

$4 - 6 \times 10^6$ yr for visible TTS. These ages had been found to be $\tau_1 = 1 - 2 \times 10^5$ yr and $\tau_2 = 1 - 2 \times 10^6$ yr by KH95. Various input parameters—such as convection, equation of state, nuclear reaction rates, and opacity can cause time shifts between different theoretical calculations. Figure 1 displays the comparison of H-R diagram of PMS stars in Taurus-Auriga with our theoretical evolutionary models. The theoretical masses range from 0.1 M_{\odot} up to 2.5 M_{\odot} ; most stars have contraction ages between 10^5 and 10^7 yr. In this region, a few stars lie very close to or on the main sequence. These stars may be actual members of the Taurus-Auriga association or they may simply be older stars sharing the same motion of the cloud members. These stars which reached post MS can be seen in comparison to derived mass distribution function with other functions.

The input physics of theoretical evolutionary models is as follows: OPAL opacity has been used and the ratio of mixing length to scale height has been taken as 1.74. The accepted chemical composition is $X = 0.699$ and the heavy metal abundance is $Z = 0.019$. When these parameters are used, the present theoretical solar model fits well to the observational values (Yıldız & Kızıloğlu 1997). Synthetic H-R diagrams of these models have been derived using different transformation tables by Akkaya & Küçük (2005). The linear interpolation method has been used in theoretical H-R diagrams for mass and age estimation of TTS. It is based on a comparison of the star's position in the T_{eff} , $\log L/L_{\odot}$ diagram with the theoretical evolutionary tracks (TET) of stars of different masses. The method follows the principle of the geometric similarity of the tracks at a given stage of evolution, which enables one to divide every TET into the same number of small intervals. Between the boundaries of equivalent intervals of the two closest TET the following conditions are satisfied (Sagar et al. 1986):

$$T_{\text{eff}} \propto M/M_{\odot}, \quad (1)$$

$$L/L_{\odot} \propto M/M_{\odot}, \quad (2)$$

$$t \propto M/M_{\odot}, \quad (3)$$

where t is the age of the star, and M/M_{\odot} is its mass in solar mass. On the other hand, for a given TET between the boundaries of a particular interval the following relation can be written:

$$L/L_{\odot} \propto T_{\text{eff}}. \quad (4)$$

Then, our theoretical models extended to the 0.1 – 2.5 M_{\odot} mass interval which contains all TTS. A linear extrapolation method is used for the age estimation of stars which lie below the evolutionary tracks. Figure 2 displays the comparison of theoret-

TABLE 1
OUR AGE AND MASS ESTIMATIONS FOR TTS

Star	M/M_{\odot}	Age	Star	M/M_{\odot}	Age
HBC 351	0.83	2.06×10^7	XZ Tau	0.46	3.95×10^4
HBC 352	1.64	6.87×10^7	HK Tau	0.51	2.56×10^6
HBC 353	1.32	1.80×10^7	J1-665	0.20	5.48×10^6
HBC 354	0.89	3.73×10^7	V710 Tau A	0.57	5.87×10^6
HBC 355	1.94	1.00×10^6	V710 Tau B	0.32	2.82×10^6
HBC 357	0.90	4.29×10^7	L1551-51	0.67	9.27×10^6
HBC 358	0.31	5.07×10^6	V928 Tau	0.52	4.40×10^6
HBC 359	0.36	4.35×10^6	V827 Tau	0.68	2.64×10^6
HBC 360	0.26	1.07×10^7	V826 Tau	0.70	2.45×10^6
HBC 361	1.26	1.07×10^7	FY Tau	0.70	2.45×10^6
HBC 362	0.28	5.95×10^6	GG Tau	0.72	7.62×10^5
LkCa 1	0.50	1.51×10^6	UZ Tau/e	0.54	2.29×10^6
Anon 1	0.68	1.98×10^6	UZ Tau/w	0.33	2.38×10^6
V773 Tau	0.74	6.64×10^5	JH 112	0.69	2.99×10^6
FM Tau	0.51	7.69×10^5	L1551-55	0.65	1.45×10^7
FN Tau	0.24	8.56×10^5	GH Tau	0.61	1.98×10^6
CW Tau	1.30	1.61×10^6	V807 Tau	0.74	1.74×10^5
LkCa 3	0.70	6.19×10^5	V830 Tau	0.69	5.64×10^6
FP Tau	0.27	1.54×10^6	GI Tau	0.78	1.25×10^6
FO Tau	0.36	4.12×10^6	GK Tau	0.72	9.17×10^5
CX Tau	0.45	6.74×10^5	DL Tau	0.70	5.14×10^5
CIDA-2	0.22	2.62×10^6	HN Tau	0.83	1.04×10^7
LkCa 4	0.36	2.48×10^6	IT Tau	1.41	7.45×10^6
CY Tau	0.50	6.85×10^5	CI Tau	0.70	1.69×10^6
LkCa 5	0.68	3.10×10^6	DM Tau	0.50	6.02×10^6
CIDA-3	0.28	5.24×10^6	J2-2041	0.23	5.58×10^6
V410 Tau	0.57	2.84×10^6	JH 108	0.41	6.96×10^6
DD Tau	0.53	1.55×10^6	HBC 407	1.15	5.15×10^7
CZ Tau	0.44	7.15×10^5	AA Tau	0.70	2.19×10^6
HBC 372	0.60	1.63×10^7	HO Tau	0.50	8.04×10^6
V892 Tau	0.16	2.05×10^6	FF Tau	0.68	8.41×10^6
Hubble 4	0.54	1.25×10^6	DN Tau	0.69	1.87×10^6
HBC 376	1.67	1.33×10^7	CoKu Tau/3	0.40	8.94×10^5
FQ Tau	0.36	4.35×10^6	HBC 412	0.57	8.30×10^5
BP Tau	0.67	2.19×10^6	HP Tau	1.30	2.84×10^6
V819 Tau	0.70	2.73×10^6	HP Tau/G3	1.65	7.06×10^5
LkCa 7	0.68	2.64×10^6	HP Tau/G2	0.60	1.33×10^7
J2-157	0.12	1.18×10^7	Haro 6-28	0.30	1.94×10^5
I04187+1927	0.62	2.90×10^6	LkCa 14	0.50	1.67×10^6

ical isochrones with TTS. By using the relation of mass and luminosity with age an age estimation is performed. Table 1 shows the age and mass estimations of all TTS obtained from theoretical evolutionary calculations of Küçük, Kızıloğlu, & Civelek (1998).

3. IMFS OF T-TAURI STARS

The theoretical evolutionary models of low mass stars in the mass range between $0.1 - 2.5 M_{\odot}$ are fitted to TTS theoretical values as displayed in Figure 3. The mass function dN is found from number of stars between $\log m$ and $\log m + 1$ mass interval.

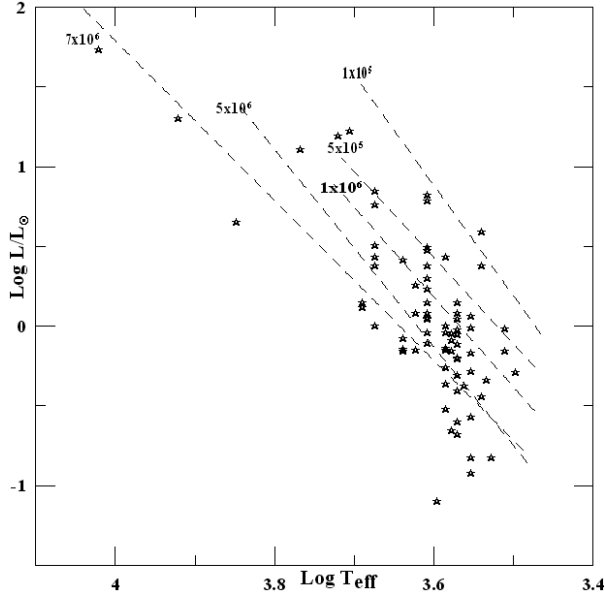


Fig. 2. Comparison of Theoretical isochrones with TTS. The crossing of 5 and 7 Myr lines is due to exceeding the valid range of the linear fit.

Here $m = M/M_{\odot}$, and M is the mass of a star and all logarithms are decimal in the paper. By using stellar data, the slope of mass function is calculated as $x=0.644\pm 0.348$, where:

$$\log N = -x \log m + \text{constant} . \quad (5)$$

We obtained a linear fit, and hence the slope of the mass function, calculated as $x = 0.644 \pm 0.348$. Here $x = \alpha - 1$ and $\xi(m) = km^{-\alpha}$ where k is a normalisation constant that depends on the total number of stars being counted. $\xi(m)$ is the number of stars per pc^3 between m , and $m + dm$ (Lequeux 1979).

The histogram on Figure 3 gives the mass distribution of TTS from theoretical evolutionary models. After the masses of stars were obtained from models, the mass distributions between $0.1-2.5 M_{\odot}$ were analysed taking $0.01 M_{\odot}$ intervals. Figure 4 displays the derived age distribution from theoretical models. As seen in this figure, most of the stars are in the $1 - 3 \times 10^6$ yr mass interval, which is the current age interval for TTS. The distance modulus (DM) of TTS in the Taurus Auriga molecular cloud is taken as $6^m.00$, resulting in $d = 140\text{pc}$. The total volume of the stars which have $M_{\text{pg}} = +9.5$ is considered to be 377pc^3 in this region.

The initial mass function [$\xi(m)$] is being considered as the number of stars in the mass interval $m \in [m, m + dm]$ per unit pc^3 . Here $dm = 0.01 M_{\odot}$, and $\xi(m)$ is calculated in the mass interval

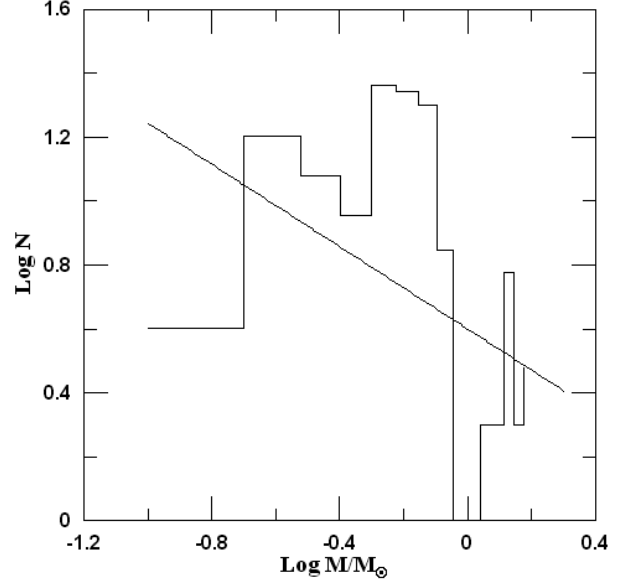


Fig. 3. The distribution of TTS in $0.1 - 1.5 M_{\odot}$ mass interval.

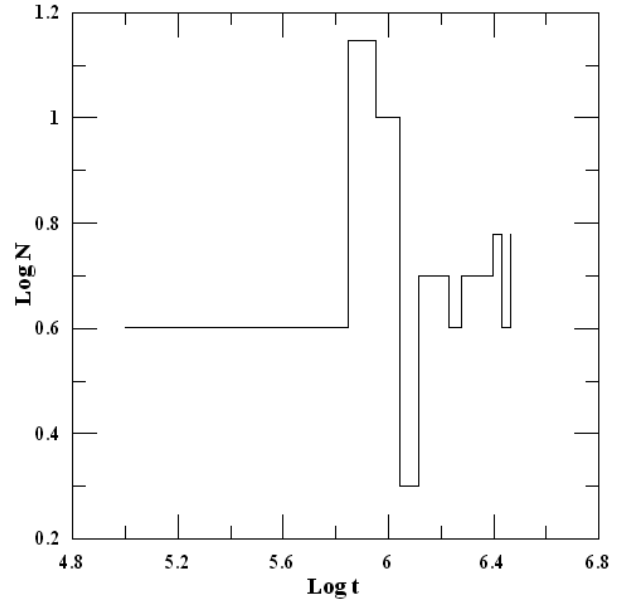


Fig. 4. Age estimations from Theoretical Models.

$0.1 - 2.5 M_{\odot}$. The IMF has different forms, in general. The logarithmic mass function ξ_L is used and the transformation to ξ is as follows:

$$\xi(m) = \frac{\xi_L(m)}{2h(m)m \ln 10} , \quad (6)$$

where $\xi(m)_L$ is the number of stars per pc^3 between $\log_{10} m + d \log_{10} m$, and $h(m)$ is the local

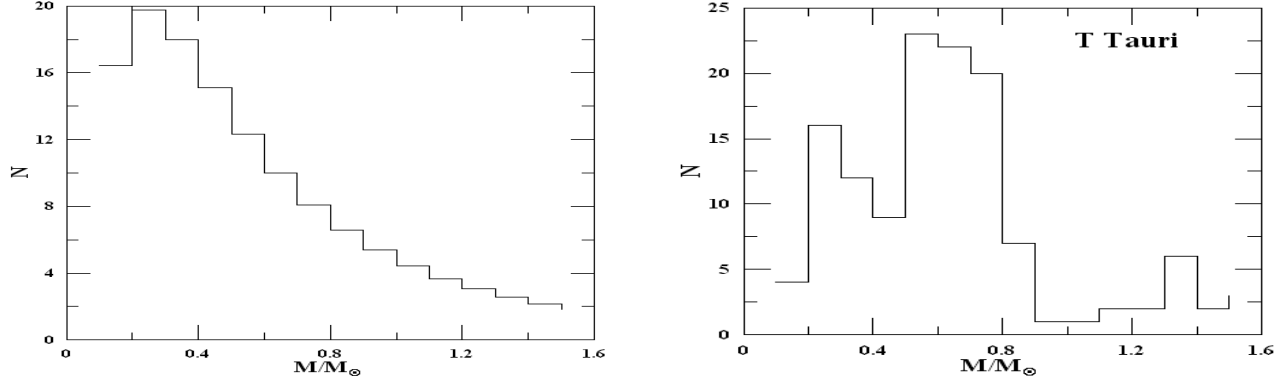


Fig. 5. The comparison of derived mass function of our theoretical isochrones and Miller & Scalo (1979). The mass distribution of Miller & Scalo (1979) (on the left) and TTS (on the right).

TABLE 2
COMPARISON OF TTSS IMF AND
MILLER & SCALO IMF

M/M_{\odot}	$\log \xi(\log m)$ (Miller & Scalo)	$\log \xi(\log m)$ (TTS)
0.1	0.57950	0.16599
0.2	0.95972	1.06907
0.3	1.09570	1.12021
0.4	1.14458	1.12022
0.5	1.15329	1.62461
0.6	1.14077	1.68449
0.7	1.11609	1.71004
0.8	1.08412	1.31210
0.9	1.04768	0.51816
1.0	1.00847	0.56392
1.1	0.96760	0.90634
1.2	0.92577	0.94413
1.3	0.88350	1.45601
1.4	0.84110	1.01107
1.5	0.79878	1.21713

scale height of the Galactic disc in the vertical direction, as a function of stellar mass. This is taken as $h=300$ pc for our mass and magnitude interval. The comparison of the derived logarithmic initial mass function of our models and the one given by Miller & Scalo (1979) is displayed in Table 2 and shown in Figure 5.

The formulation of Kroupa, Tout, & Gilmore (1990, 1991) of the mass function of Miller & Scalo (1979) is:

$$p_i = C \exp\left[-\frac{(\log M_i - \log \mu)^2}{2(\log \sigma)^2}\right], \quad (7)$$

where $\mu=0.23$ and $\sigma=0.42$. In both IMFs, the constant C is determined from

$$\sum_{i=1}^{N_m} f_i = 1. \quad (8)$$

The number of stars per magnitude bin is then $N_i = N_{\star} f_i$, where N_{\star} is the total number of stars in the sample. This value is 200 for our sample (KH95). The probability of finding a star with a final mass between M_i and M_{i+1} is given by

$$f_i = 0.5(p_i + p_{i+1}). \quad (9)$$

Here, p_i and p_{i+1} are the probabilities of finding a star with a final mass M_i , and M_{i+1} , respectively. By the way, the probability and number of these stars have been computed in the mass interval of M_i and M_{i+1} (in fact $(M_{i+1} - M_i)$ is used to define the stars between M_i and M_{i+1} , not to define mass, as can be seen in Appendix B of KH95). As compared with Miller & Scalo (1979) and TTS, the fit decreases with increasing mass. This is a result of the discrepancy between the Miller & Scalo (1979) IMF which is for MS stars and our models' IMF, which is for PMS stars. These results are in good agreement and coincident with the Miller & Scalo (1979) and Salpeter (1955) IMF values. As seen in Figure 6, the maximum of the IMF is around $0.4 M_{\odot}$ which is in good agreement with the Miller & Scalo (1979) IMF. Here we used polynomial fit

$$\log \xi(\log M/M_{\odot}) = 1.176 - 1.150 \log M/M_{\odot} - 2.09(\log M/M_{\odot})^2. \quad (10)$$

However, TTS are in the PMS stage of their evolution and also there are invisible stars in that region. The results of this paper agree with KH95 which uses

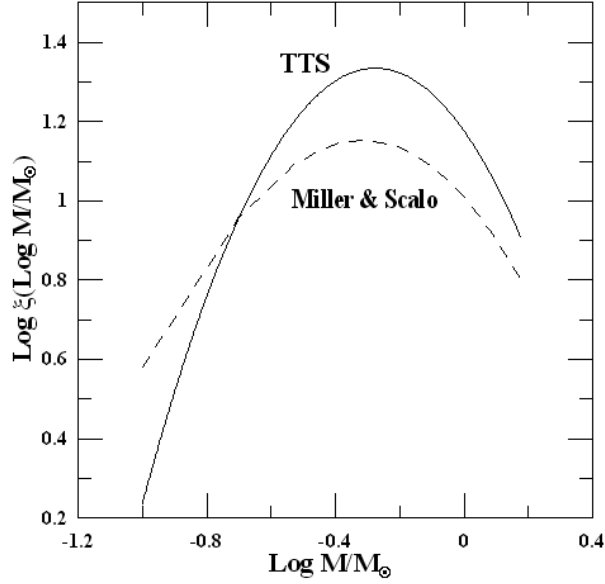


Fig. 6. Comparison of $\xi(\log m)$ logarithmic mass functions.

two distinct theoretical models. The best feature of Figure 6 is the maximum of the IMFs at $0.4 M_{\odot}$. But our IMF value is larger than that of the Miller & Scalco IMF

$$\Delta \log \xi(m) = 0.18, \quad (11)$$

both reaching a maximum at around -0.4 within small differences.

In the literature there exist calculations of IMFs, especially for high mass stars. The IMF calculations for open clusters seem to be more trustworthy. Miller & Scalco (1979) ($M > 10 M_{\odot}$) and Lequeux (1979) ($M > 2 M_{\odot}$) have found a sharper slope for IMFs of high mass field stars than for intermediate mass field stars.

4. RESULTS AND DISCUSSION

In this work, IMF and age estimations of TTauri stars in the Taurus-Auriga region are presented by using our theoretical evolutionary models in the mass interval $0.1 - 2.5 M_{\odot}$. We proceed by comparing theoretical to observed values of low mass stars for those TTS for which we have been able to construct a synthetic optical HR diagram. As noted

previously, we use the HR diagram to derive masses for TTS, as well as to estimate the ages. We present our results on age and mass distributions in Table 1. Our results for determining the IMF are appropriate for open clusters like NGC 2264, IC 348, but seem not to hold for open clusters having high mass stars. The slope of the IMF for TTS is found to be $x = 0.644 \pm 0.348$ and the age interval is found to be $1 - 3 \times 10^6$ yrs. Unresolved binaries significantly affect the relation between the observed luminosity functions and the corresponding mass functions. Shifts in the logarithmic mass function around $0.1 - 0.2 M_{\odot}$ as compared with Miller & Scalco (1979) may be caused by unsuitable photometric data or effects of binary stars which are not taken into account. Also Thies & Kroupa (2007) state that more recent work shows a flattening in the lower mass regime of the observed mass function and in the ξ_L representation.

This work was supported by the Section of Scientific Research Projects (EUBAP) of the Erciyes University, Project number: FBT-05-36.

REFERENCES

- Akkaya, İ., & Küçük, İ. 2005, *Astron. Astrophys. Transactions*, 6, 497
- Davé, R. 2008, *MNRAS*, 385, 147
- Kenyon, S. J., & Hartmann, L. 1995, *ApJS*, 101, 117 (KH95)
- Kroupa, P. 2002, *Science*, 295, 82
- Kroupa, P., Tout, C. A., & Gilmore, G. 1990, *MNRAS*, 244, 76
- _____. 1991, *MNRAS*, 251, 293
- Küçük, İ., Kızıloğlu, N., & Civelek, R. 1998, *Ap&SS*, 3, 279
- Larson, R. B. 1999, in *Star Formation*, ed. T. Nakamoto (Nobeyama: Nobeyama Radio Observatory), 336
- Lequeux, J. 1979, *A&A*, 80, 35
- Luhman, K. L. 2004, *ApJ*, 617, 1216
- Miller, G. E., & Scalco, J. M. 1979, *ApJS*, 41, 513
- Salpeter, E. E. 1955, *ApJ*, 121, 161
- Scalo, J. M. 1986, *Fund. Cosmic Phys.*, 11, 1
- Sagar, R., Piskunov, A. E., Miakutin, V. I., & Joshi, U. C. 1986, *MNRAS*, 220, 383
- Thies, I., & Kroupa, P. 2007, *ApJ*, 671, 767
- Walter, F. M., Brown, A., Mathieu, R. D., Myers, P. C., & Vrba, F. 1988, *AJ*, 96, 297
- Yıldız, M., & Kızıloğlu, N. 1997, *A&A*, 326, 187